9th Asia-Pacific Conference on Combustion,
Gyeongju Hilton, Gyeongju, Korea
19-22 May 2013

A DNS Study of Ignition of Lean PRF/Air Mixtures under HCCI Conditions

Minh Bau Luong, Chun Sang Yoo*

School of Mechanical and Advanced Materials Engineering, Ulsan National Institute of Science and Technology (UNIST), Ulsan 689-798, Republic of Korea

Abstract

Direct numerical simulations (DNSs) of ignition of lean primary reference fuel (PRF)/air mixtures under homogeneous charge compression ignition (HCCI) conditions were performed using a 116-species reduced mechanism. The influence of fuel composition and thermal stratification on ignition characteristics of lean PRF/air mixtures is investigated. Displacement speed and Damköhler number analyses reveal that high temperature fluctuation induces deflagration waves at the reaction fronts such that mean heat release rate increases more slowly and more spread out in time, consequently preventing excessive rate of pressure rise throughout the ignition process. The propagation characteristics of deflagration waves of different PRF/air mixtures are almost the same such that the overall combustion characteristics of different PRF/air mixtures become nearly identical and thus, the effect of fuel composition on the ignition vanishes. On the contrary, for small degree of thermal stratification, spontaneous ignition prevails during the whole ignition process, and hence, those ignition characteristics are quite similar to the corresponding 0-D homogeneous auto-ignition.

1 Introduction

Homogeneous charge compression ignition (HCCI) has emerged as one of the most effective and feasible engine concepts with great potential to obtain both high diesel-like efficiency and significantly reduced specific fuel consumption with ultra-low NO_x and soot emissions. However, its operating range is rather limited and there still exist difficulties in accurately controlling ignition timing and alleviating excessive pressure rise rate under a wide range of load conditions [1, 2].

By the help of the chemical mechanism reduction techniques and the development of high performance computing (HPC) clusters, however, multi-dimensional direct numerical simulations (DNSs) of HCCI combustion of hydrocarbon fuel/air mixtures can now be simulated with realistic kinetic mechanisms and provide detailed understanding of the HCCI combustion. Chen and co-workers elucidated the effect of temperature inhomogeneities and turbulent timescale on the ignition characteristics of lean hydrogen/air mixtures under HCCI conditions [3,4]. Bansal and Im investigated the effects of composition inhomogeneities together with temperature fluctuations on the HCCI combustion of the same lean hydrogen/air mixture [5]. Yoo et al. investigated the ignition characteristics of a lean *n*-heptane/air mixture with different mean and root-mean-square (RMS) of temperature and the effect of the negative-temperature coefficient (NTC) regime on the overall HCCI combustion [6]. Recently, Yoo et al. studied the ignition characteristics of a lean *iso*-octane/air mixture with temperature fluctuations and spark-ignition timing under both HCCI and spark-assisted compression ignition (SACI) conditions [7].

Up to now, most of the previous DNS studies were focused on the effects of thermal and composition stratifications and turbulence timescales on HCCI combustion. Therefore, the objective of the present study is to understand and compare the ignition characteristics of different hydrocarbon fuel/air mixtures under HCCI conditions. For this purpose, primary reference fuels (PRFs) are chosen because they have been used to investigate the combustion characteristics of HCCI engines by the engine community.

Primary reference fuel is a mixture of *n*-heptane and *iso*-octane with the percent of *iso*-octane in volume being the index of PRF. For instance, PRF80 is composed of 80 % of *iso*-octane and 20 % of *n*-heptane by volume, respectively. Ultimately, the present study aims to provide strategies to control the rate of heat release in HCCI combustion by performing two-dimensional parametric DNSs, systematically varying two key parameters concerning mixture inhomogeneities: 1) the fuel composition and 2) the initial variance of the temperature, T'.

2 Numerical Methods and Conditions

For the present DNS study, the Sandia DNS code, S3D, was employed [8]. A new 116-species PRF/air reduced mechanism linked with CHEMKIN and TRANSPORT software libraries [9-10] was used for evaluating reaction rates and thermodynamic and mixture-averaged transport properties. As in the previous DNS studies of hydrocarbon fuel/air HCCI combustion [6-7], periodic boundary conditions were imposed in all directions such that ignitions of PRFs/air mixtures occur at constant volume.

The initial uniform equivalence ratio, ϕ, and pressure, p, are 0.3 and 20 atm, respectively. Note that $\phi = 0.3$ is adopted to elucidate the ignition characteristics of PRF/air mixtures under high load HCCI conditions. A total of nine DNS cases were performed in the parameter space of initial physical conditions: three different fuels (PRF50, PRF80, and PRF100) and temperature fluctuation root mean square (RMS), T'.

Figure 1 shows the zero-dimensional homogeneous ignition delay, τ_{ig}^0, for three different PRF/air mixtures. Note that τ_{ig} represents the time at which the maximum mean heat release rate (HRR) occurs and the superscript 0 denotes 0-D homogeneous auto-ignition. It is readily observed from the figure that the more *iso*-octane in the mixtures is, the more resistant it is to auto-ignition. At the initial temperature of 1024 K, for instance, the homogeneous ignition delays of PRF100, PRF80, and PRF50 are 2.5, 2.39, and 2.29 ms, respectively. Note that for all 2-D DNSs, the mean initial temperature, T_0, is 1024 K.

The initial turbulent flow field is prescribed by an isotropic kinetic energy spectrum function as in [6,7]. The initial temperature field is also generated by a temperature spectrum,

*Corresponding author. Fax: +82-52-217-2309
E-mail address: csyoo@unist.ac.kr

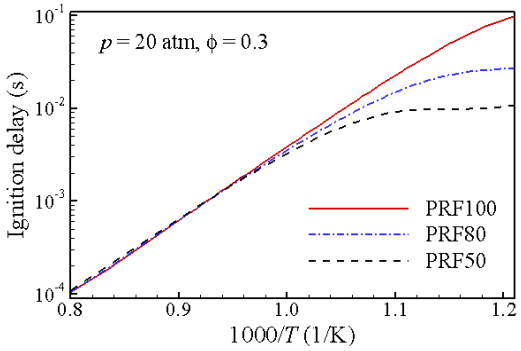

Figure 1. Homogeneous ignition delay of different PRFs at constant volume with initial pressure of 20 atm as a function of initial temperature.

similar to the kinetic energy spectrum. The turbulence intensity, u' = 2.5 m/s, most energetic turbulent length scale, l_e= 1.25 mm, and most energetic temperature length scale, l_{Te} = 1.25 mm, are used. Details of the physical parameters for each case are presented in Table 1.

The computational domain is a 2-D square box with the domain size of 3.2 mm, discretized with 640 grid points. Typical profiles of initial temperature and vorticity are shown in Fig. 2. All of the DNSs were performed on IBM Blue Gene/P at King Abdullah University of Science and Technology (KAUST) and required approximately 7 million CPU-hours.

Case	Fuel	T_0 (K)	T'(K)	τ_t (ms)	τ_{ig}^0(ms)
1	PRF100	1024	15	2.5	2.50
2	PRF100	1024	30	2.5	2.50
3	PRF100	1024	60	2.5	2.50
4	PRF80	1024	15	2.5	2.39
5	PRF80	1024	30	2.5	2.39
6	PRF80	1024	60	2.5	2.39
7	PRF50	1024	15	2.5	2.29
8	PRF50	1024	30	2.5	2.29
9	PRF50	1024	60	2.5	2.29

Table 1. Physical parameters of the DNS

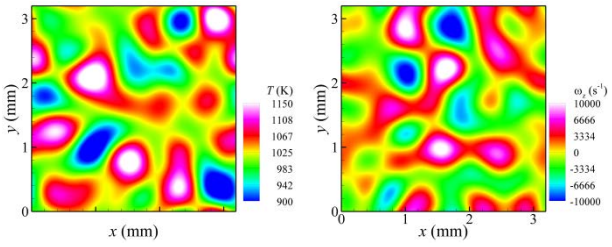

Figure 2. Initial profiles of temperature and vorticity for Case 9

3 Results and Discussion

3.1 Overall Combustion Characteristics

Nine DNS cases were performed to elucidate the effect of temperature fluctuations on the ignition characteristics of the different PRF/air mixtures. Three different degrees of temperature fluctuation are chosen: T' = 15, 30, and 60 K. Figure 3 shows the temporal evolution of the mean pressure, $\bar{p}$, and the mean heat release rate, $\bar{\dot{q}}$. The corresponding zero-dimensional homogeneous auto-ignitions are also shown in the figure for comparison. The time is normalized by the 0-D homogeneous ignition delay of PRF100/air mixture of τ_{ig}^0 = 2.5 ms

As shown in Fig. 3, the mean pressure increases more slowly and the mean heat release rate becomes smother with increasing T' regardless of the fuel composition. The overall combustion is also advanced with increasing T'. These ignition characteristics are qualitatively identical to those of ignition Characteristics of the hydrogen/air, *n*-heptane/air, and *iso*-octane/air mixtures with high mean initial temperature [3–7].

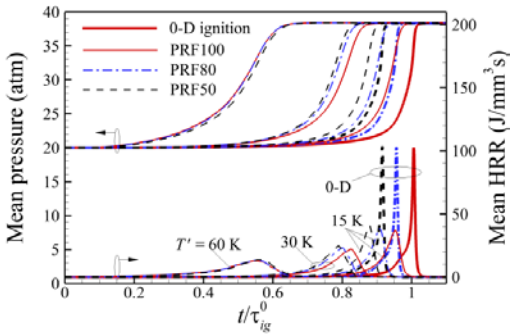

Figure 3. Temporal evolution of the mean pressure and the mean heat release rate. Thick lines represent the corresponding cases of 0-D homogeneous ignition.

For cases with small T' (Cases 1, 4, 7), ignition delay, τ_{ig}, increases with increasing *iso*-octane volume percent in the PRF (PRF50 → 80 → 100) like 0-D homogeneous auto-ignition. Moreover, the duration of the combustion is much shorter, and the peak $\bar{\dot{q}}$ is much larger than those of cases with large T'. These results suggest that for small T', the overall combustion occurs primarily through spontaneous ignition and hence, the ignition characteristics of 2-D DNS cases become similar to those of 0-D homogeneous auto-ignition.

On the contrary, for large T' (Cases 3, 6, 9), the temporal evolutions of $\bar{\dot{q}}$ are nearly identical for the three cases in spite of different PRF compositions, implying that the effect of different fuel compositions of PRFs on ignition becomes negligible. It is also readily observed from Fig. 3 that for cases with large T', the start of ignition occurs sooner and the duration of combustion process persists longer compared with the cases with low T'. These results implies that large T' can prevents the excessive rate of pressure rise by promoting spreading of the mean heat release rate.

To further examine the mode of combustion, isocontour of heat release rate, $\dot{q}$, for Cases 1–3 is shown in Fig. 4 at each τ_{ig}. $\dot{q}$ is normalized by the maximum $\dot{q}$ of the 0-D homogeneous ignition of PRF100/air mixture, $\dot{q}_m^0$ = 103.5 Jmm^3/s. It is readily observed from the figure that for small T' (Case 1), $\dot{q}$ occurs nearly simultaneously over a wide area of domain as spontaneous ignition. For large T' (Case 3), however, high $\dot{q}$ occurs primarily in thin reaction fronts and relatively small $\dot{q}$ occurs over a broader area, suggesting that the overall combustion in large T' cases occurs through the mixed mode of deflagration and spontaneous ignition. Therefore, for large T' cases, the characteristics of flame propagation, or the turbulent flame speed is supposed to play a critical role in determining the overall combustion.

For better understanding of ignition characteristics, four snapshots of isocontour of normalized heat release rate at different times are shown for PRF100 with T' = 15 K (Fig. 5) and 60 K (Fig. 6). As shown in Fig. 5 (PRF100 with T' = 15 K), the mixture burns spontaneously with the very short duration of combustion.

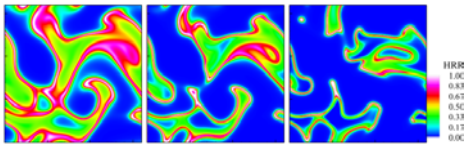

Figure 4. Isocontours of normalized HRR for Cases 1-3 (from left to right) at t/τ_{ig}^0 = 0.95, 0.82, and 0.56, respectively.

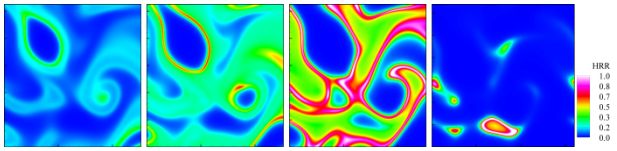

Figure 5. Isocontours of normalized heat release rate for Case 1 (from left to right) at t/τ_{ig}^0 = 0.90, 0.93, 0.95 and 0.98.

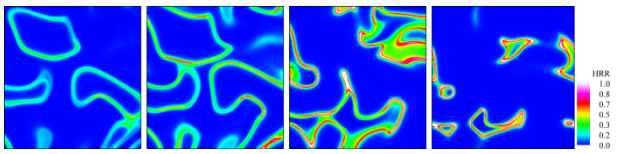

Figure 6. Isocontours of normalized heat release rate for Case 3 (from left to right) at t/τ_{ig}^0 = 0.40, 0.48, 0.56 and 0.60.

For T' = 60 K (Case 3), however, it is readily observed that the larger initial temperature fluctuation induces several ignition spots which develop into deflagration waves and most heat release occurs in thin reaction sheets, implying that the deflagration waves advance the overall combustion and significantly increase the duration of the combustion. As a result, the heat release rate is effectively smoothed out.

Note that in the present study, an identical initial turbulence field is used for all 2-D DNSs and hence, only the laminar flame speed can effectively change the turbulent flame speed. Note also that the laminar flame speeds of different PRFs in the present study are nearly identical (not shown here). As such, the combustion phase of the three cases would be the same only if the initial ignition kernels are not affected significantly by the turbulence field.

These results imply that for large T' cases, the effect of different fuel composition or chemistry of PRF/air mixtures on the ignition characteristics of PRF HCCI combustion vanishes because the deflagration mode of combustion is predominant at the reaction fronts. This may justify that HCCI engines can operate on various types of fuels with appropriate methods in controlling ignition timing and the spreading of heat release rate.

3.2 Font Speed and Burning Rate

To qualitatively distinguish between spontaneous ignition and deflagration modes of combustion, the density-weighted displacement speed, S_d^*, is adopted to delineate between two combustion modes. S_d^* is defined by:

$$S_d^* = \frac{1}{\rho_u |\nabla Y_k|}\left(\dot{\omega}_k - \nabla \cdot (\rho Y_k \boldsymbol{V}_k)\right), \qquad (1)$$

where Y_k, $\boldsymbol{V}_k$, and $\dot{\omega}_k$ denote species mass fraction, species diffusion velocity in the j-direction and net production rate of species k, respectively, and ρ_u is the density of the unburnt mixture. ρ_u is calculated from the local enthalpy and fresh mixture condition assuming pressure and enthalpy remain constant across the front. In the present study, the isocontour of $Y_c = Y_{CO_2} + Y_{CO} =$ 0.049 is chosen to evaluate the displacement speed for all cases.

Figure 7 shows the temporal evolution of S_d^* for 1-D reference cases and the mean front speed, $\overline{S_d^*}$, for 2-D DNS cases, all of which are normalized by the corresponding 1-D laminar flame speed, S_L, which is estimated from a transient one-dimensional reactive simulation. The simulation was initialized with a high-temperature ignition source such that a combustion wave emanates from the source, propagating into the reactive mixture ahead of it. From the simulations, S_L is found to be approximately 0.37 m/s for all PRF/air mixtures. It is readily observed from Fig. 7 that the mean front speeds exhibit a characteristic 'U' shape qualitatively consistent with previous studies [6,7]. The occurrence of the 'U'-shaped mean front speed is attributed to the initial thermal run-away in the nascent ignition kernel during the early phase of combustion and the burnout of remaining charge due to compression heating during the last phase of combustion [6,7].

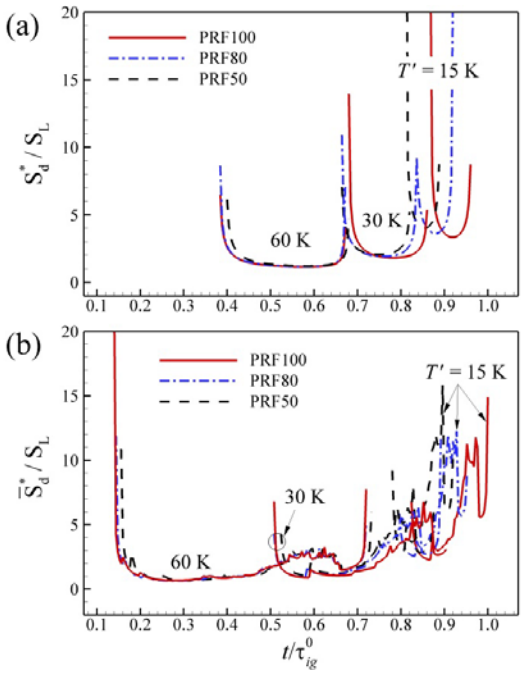

Figure 7. Temporal evolution of (a) the front speed, S_d^*, for one-dimensional reference cases (b) the mean front speed, $\bar{S}_d^*$, for two-dimensional DNS cases with different temperature RMS and different PRFs.

It is readily observed from the figure that the mean front speed similar to S_L develops earlier with increasing T' and the duration of the region of constant front speed at the bottom of the `U' shape also increases with increasing T'. For cases with small T', however, the mean front speed is much greater than S_L and there is no region of constant front speed. These results

imply that for cases with large T', combustion at the reaction fronts occurs primarily by deflagration rather than by spontaneous ignition. On the contrary, for cases with small T', a small degree of thermal stratification leads an excessive rate of heat release due to simultaneous auto-ignition occurring throughout the whole domain, which should be avoided in HCCI combustion. These results also suggest that the critical degree of thermal stratification for smooth operation of HCCI engines depends largely on the temperature fluctuation, T', such that the effects of different chemical compositions in fuels are hence reduced. On that account, it is crucial to consider the role of the temperature fluctuation, T', to ensure a moderate pressure rise rate.

Another quantitative means to measure the occurrence of deflagration and spontaneous ignition modes of combustion, Damköhler number is adopted to find the contribution of heat release from deflagration mode. Damköhler number, *Da*, is defined by:

$$Da = \frac{\dot{\omega}_k}{\left|-\nabla \cdot (\rho Y_k \boldsymbol{V}_{j,k})\right|}, \qquad (2)$$

where Y_c is used to evaluate *Da*. From 1-D simulations, *Da* is found to be approximately 3.3 in the diffusive limit. The diffusive limit represents deflagration wave propagation without auto-ignition; i.e., where diffusion balances reaction. For *Da* less than 3.3, combustion occurs by deflagration.

Figure 8 shows the temporal evolution of the fraction of heat release rate attributed by deflagration for Cases 1–9 together with the mean heat release rate.

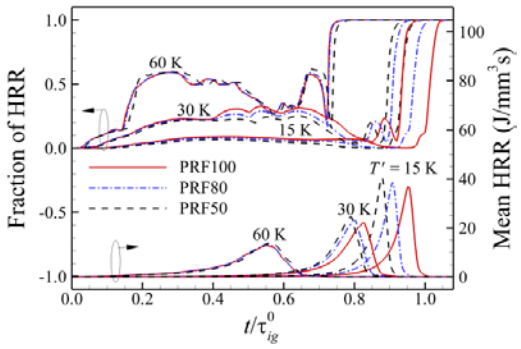

Figure 8. Temporal evolution of fraction of heat release rate from the deflagration mode and HRR with different temperature RMS and different PRFs.

As shown in Fig. 8, the fraction of heat release rate from deflagration increases significantly with increasing T' regardless of the fuel composition. For cases with small T', the total heat release from the deflagration mode of combustion is only about 1%, implying that spontaneous auto-ignition prevails throughout the whole combustion process. On the contrary, for cases with large T', total heat release from deflagration is more than 40 % of total heat, indicating that the deflagration mode of combustion can temporally spread out the heat release rate and advance the overall combustion. It is also observed from Fig. 8 that for large T', even at the peak heat release rate, the deflagration wave still exists. However, the deflagration mode of combustion does not occur for cases with small T', solely spontaneous wave happens. These results also verify that deflagration is attributed to spreading out the heat release rate.

4 Conclusions

The effects of thermal stratification and fuel composition on ignition of lean PRF/air mixtures under HCCI conditions were investigated using direct numerical simulations with a new 116-species reduced mechanism for PRF oxidation. The nine 2-D DNSs were carried out with different degrees of temperature fluctuations for three different PRF/air mixtures. The results show that, in general, larger T' induces greater temporal spreading of the mean heat release rate due to the predominance of deflagration mode at the reaction fronts and hence, the physical properties (ex. flame speed, diffusivities) rather than chemistry of the fuel/air mixture become more important in determining the combustion characteristics. As such, the effect of the fuel composition on ignition characteristics of PRF/air mixtures vanishes with increasing T'. On the contrary, spontaneous ignition mode prevails for small T' such that the effect of fuel compositions or chemistry remaining in the overall ignition are more important than the physical properties of the fuel/air mixtures.

5 Acknowledgment

This work was supported by Basic Science Research Program through the National Research Foundation of Korea (NRF) funded by the Ministry of Education, Science and Technology (No. 2012-0003222) and the Human Resources Development of the Korea Institute of Energy Technology Evaluation and Planning (KETEP) grant funded by the Korea government Ministry of Knowledge Economy (No. 20114030200010). The authors would like to thank Prof. T. Lu and Dr. Z. Luo of Univ. of Connecticut for providing the 116-species PRF/air reduced mechanism. This research used the resources of the Supercomputing Laboratory at King Abdullah University of Science and Technology (KAUST). The authors would like to acknowledge the help of Prof. F. Bisetti at KAUST for this project.

References

[1] J. Dec, Proc. Combust. Inst. 32 (2009) 2727–2742.
[2] M. Yao, Z. Zheng, and H. Liu, Prog. Energy Combust. Sci. 35 (2009) 398–437
[3] J.H. Chen, E.R. Hawkes, R. Sankaran, S.D. Mason, H.G. Im, Combust. Flame 145 (2006) 128–144.
[4] E.R. Hawkes, R. Sankaran, P. Pébay, J.H. Chen, Combust. Flame, 145 (2006) 145–159.
[5] G. Bansal, H.G. Im, Combust. Flame 158 (2011) 2105-2112.
[6] C.S. Yoo, T. Lu, J.H. Chen, C.K. Law, Combust. Flame 158 (2011) 1727-1741.
[7] C.S. Yoo, Z. Luo, T Lu, H. Kim, J.H. Chen, Proc. Combust. Inst. 34 (2013) 2985-2993.
[8] J.H. Chen, A. Choudhary, B. de Supinski, M. DeVries, E.R. Hawkes, S. Klasky, W.K. Liao, K.L. Ma, J. Mellor-Crummey, N. Podhorszki, R. Sankaran, S. Shende, C.S. Yoo, Comput. Sci. Disc. 2 (2009) 015001.
[9] R.J. Kee, F.M. Rupley, E. Meeks, J.A. Miller, CHEMKIN-III, Tech. Rep. SAND96-8216, Sandia National Laboratories, 1996.
[10] R.J. Kee, G. Dixon-Lewis, J. Warnatz, M.E. Coltrin, J.A. Miller, Tech. Rep. SAND86-8246, Sandia National Laboratories, 1986.